Int. J. Electrochem. Sci., 7 (**2012**) 3527 - 3536

International Journal of
ELECTROCHEMICAL
SCIENCE
www.electrochemsci.org

5-Aminotetrazole as a Corrosion Inhibitor in a Phosphate Cu ECMP Electrolyte

Jeng-Yu Lin[*] *and Shu-Wei Chou*

Department of Chemical Engineering, Tatung University, Taipei, 104 Taiwan
[*]E-mail: jylin@ttu.edu.tw

Received: 24 November 2011 / *Accepted:* 16 March 2012 / *Published:* 1 April 2012

In this study, 5-aminotetrazole (ATRA) was characterized as a corrosion inhibitor in a phosphate electrolyte for Cu electrochemical mechanical planarization (ECMP). The D.C. and A.C. electrochemical results revealed that ATRA can inhibit Cu surface against dissolution more effectively compared to benzotriazole (BTA). A potential window (~ 0.4 V) within which the planarization efficiency and the Cu removal rate were greater than 70% and 600 nm min^{-1}, respectively, was obtained. It was also found that ATRA stood up lengthwise on the Cu surface, thus resulting in the formation of dense possible polymer film. Consequently, the enhanced passivation capability of ATRA could be attributed to the dense possible polymer film. The ECMP polishing results also presented that a step height reduction of ~800 nm can be achieved at such high potential of 0.7 V vs. Ag/AgCl for only 60 s while 0.01 M ATRA was employed.

Keywords: Electrochemical Mechanical Planarization, Corrosion Inhibitor, Phosphate Electrolyte

1. INTRODUCTION

Electrochemical mechanical planarization (ECMP) has been widely considered an alternative capable of conventional chemical mechanical planarization (CMP) process due to its advantages of high planarization efficiency and enhanced removal rate achieved at low downward-pressure, the simplification of end-point detection, and the reduction of consumables use [1-6]. Previously, we have proposed an oxidizer-free phosphate electrolyte containing benzotriazole (BTA) for Cu ECMP process at low downward-pressure [6,7]. BTA acted as a corrosion inhibitor and was employed to enhance the planarization efficiency due to the formation of BTA passive films [8,9]. Nevertheless, it was found that BTA passive films were only stable at low operating potentials in the phosphate ECMP electrolyte, resulting in a narrow operating potential window and a relative low removal rate [6,7]. The low removal rate can lead to a long polishing time. Typically, a Cu CMP is required to remove residual

metal after Cu ECMP process when using a nonconductive polishing pad [10]. It is critical to diminish polishing time to balance polishing steps in a serial mode over multiple platens. The time balancing is crucial to prevent waiting between steps, thus could be helpful with throughput and corrosion defectivity reduction in the planarization process. Consequently, the enhancement of inhibitor capability is critical to expand the operating potential window, thus resulting in the increase in removal rate and the decrease in polishing time during ECMP.

Lee et al [11]. proposed that 5-aminotetrazole (ATRA) was a more effective corrosion inhibitor compared to BTA for use in Cu CMP slurries. Therefore, this present article is first intended to investigate the planarization capability and removal rate of a phosphate ECMP electrolyte containing ATRA as an inhibitor. The voltammetry and electrochemical impedance spectroscopy were used to characterize the inhibition capability of ATRA passive film at various anodic potentials. The atomic force microscopy (AFM) measurements were utilized to characterize the morphologies of inhibitors adsorbed on the Cu surface. Thus patterned Cu foils were further employed to study the planarization efficiency while using the phosphate electrolyte containing ATRA.

2. EXPERIMENTAL

2.1. Electrolyte and sample preparation

The phosphate electrolyte was prepared by referring to our previous studies [6,7]. De-ionized water and reagent-grade chemicals were used to prepare a phosphate electrolyte consisting of 1 M potassium phosphate (monobasic, Sigma Aldrich). The pH value was adjusted to 2 by means of small amounts of pure ortho-phosphoric acid (85%, Merck). BTA (TCI America) and ATRA (TCI America) served as inhibitors in the phosphate electrolytes. Cu foil (99.99% purity) obtained from Sigma Aldrich was washed several times in 20% NaOH solution containing 200 g/L zinc dust until clean [12]. It was further electropolished at a constant potential of 1.2 V vs. Ag/AgCl for 1 h to reduce its surface roughness and remove the air-formed oxides on its surface, followed by the following desired measurements.

2.2. Electrochemical measurements

Linear voltammetry measurements with and without abrasion were conducted using an electrochemical analyzer system, CHI 614D (CH Instruments, USA). A fragment of the electropolished Cu foil (1 cm^2) mounted onto the rotating disk electrode (RDE) adaptor functioning as a working electrode. An electrochemical test cell was employed, basically following our previous design [13]. The polishing platform had four triangular notches along the sides; thus the electrolyte in direct contact with the Cu foil or Cu patterned structure could mix with, and be replenished by, fresh bulk electrolyte during polishing. The IC1000™ pads were used as the polishing pads and the downward force was controlled at ~0.5 psi during polishing. The EIS measurements were performed using an IM-6 impedance analyzer (IM6, Zahner). A 5 mV amplitude sinusoidal wave was applied in

the tested frequency range of 10 Hz–100 kHz. For each potential step, the electrode was allowed to stabilize for 10 min before performing measurements. The IM-6ATHALES software package was used for acquisition and analysis of impedance spectra, and simulation of equivalent circuit. A platinum wire and saturated silver/silver chloride (Ag/AgCl) electrode were assembled as a counter and a reference electrode, respectively for the aforementioned electrochemical measurements.

2.3. Characteristics of passive films

As for the characteristics of passive films, the surface morphologies of Cu foils covered with passive films was characterized by an atomic force microscopy (NS3a controller with D3100 stage; Digital Instruments) in tapping mode at a scan rate of 0.5 Hz.

2.4. Polishing experiments

A Cu foil (1 cm^2) with patterned structure was mounted onto the adaptor for polishing. The detailed fabrication for the patterned Cu foils is described in our previous study [14]. The profile of the pattern was recorded to monitor changes caused after ECMP process by using a surface profiler (Dektak 150, VEECO). The depth of the features was measured at ~2.5μm before ECMP process. It should be noted that the trenches were not uniform as shown in the profilometric scans. This edge effect may be anticipated by considering the solution conductivity, with the current density near the edge much higher than in the center during the electropolishing steps. Thus the edge effect did not be attributed to the ECMP process [15].

3. RESULTS AND DISCUSSION

3.1. Potentiodynamic curves

The voltammetry curves shown in Fig. 1 demonstrate the change in current density (with and without abrasion) for phosphate electrolytes containing 0.01 M BTA and 0.01 M ATRA, respectively. The voltammetry curve with abrasion corresponds to the Cu removal rate obtained from the surface elevations in contact with the pad, while the voltammetry without abrasion represents the Cu removal rate within the surface recesses. The large discrepancy in current densities between the abrasion curve and non-abrasion curve can be observed for both electrolytes. It can be noted that the rate of Cu dissolution was significantly enhanced with pad abrasion. Figure 1 also demonstrates that the desorption of BTA and ATRA from the Cu surface ~0.5 V and ~0.75 V vs. Ag/AgCl respectively. At this voltage, the Cu surface is no longer protected against dissolution by either inhibitor.

Additionally, the Cu removal rate can be similarly proportional to the applied external current via Faraday's law according to the previous study [3]. The voltammetry curves with abrasion shown in Fig. 1 can be employed to calculate the Cu removal rate during ECMP, as shown in Fig. 2. Furthermore, a removal rate within the surface recesses corresponds to the non-abrasion curve.

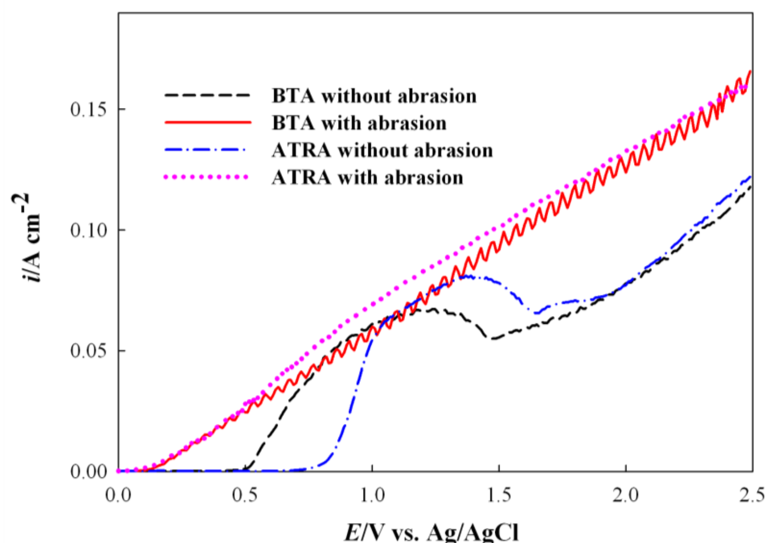

Figure 1. Anodic polarization curves measured with and without abrasion in phosphate electrolytes consisting of 0.01 M BTA or 0.01 M ATRA. The sweep potential was performed from 0 V to 2.0 V vs. Ag/AgCl at a scan rate of 5 mV s^{-1}. Rotation speeds of 100 rpm were used during the measurements.

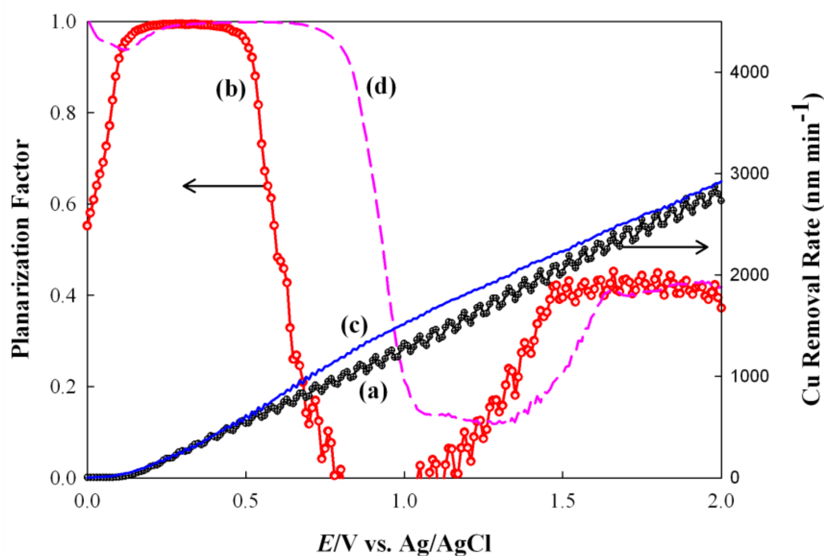

Figure 2. Calculated Cu removal rate and planarization factors defined by Eq. (1) as a function of potential for phosphate electrolytes containing 0.01 M BTA or 0.01 M ATRA.

As a result, a planarization factor, ε_{ECMP}, can be defined as following [3,5,6]:

$$\varepsilon_{ECMP} = \frac{i_{abrasion} - i_{no \quad abrasion}}{i_{abrasion}} \qquad (1)$$

Thus, the ε_{ECMP} for phosphate electrolyte containing BTA or ATRA can be obtained and illustrated in Fig. 2. Tripathi et al. [5] proposed that a desirable ECMP process would have a removal rate of 600 nm/ min and $\varepsilon_{ECMP} > 70\%$. The values of ε_{ECMP} over 70% were observed until 0.6 V and 0.9 V vs. Ag/AgCl for electrolytes containing 0.01 M BTA and 0.01 M ATRA, respectively. Additionally, the removal rate > 600 nm/ min was found while the sweep potential reached 0.5 V vs. Ag/AgCl for both electrolytes. These results indicate that a wider effective potential window (~ 0.4 V) can be obtained for the electrolyte containing 0.01 M ATRA compared to that containing 0.01 M BTA (~0.1 V).

3.2. EIS tests

To further evaluate the passivation capability of inhibitors in the phosphate electrolytes, EIS analyses were also carried out. Figures 3a and 3b show Nyquist plots for the impedance spectra of Cu foils as a function of applied potential in the phosphate electrolyte containing 0.01 M BTA and 0.01 M ATRA, respectively. The measured impedance results were analyzed on the basis of the equivalent circuit model shown in Fig. 3c. The model circuit consists of four elements: the iR (R_s), the charge-transfer resistance (R_{ct}), the constant phase element (CPE) used in place of double-layer capacitance; and the Warburg impedance (*W*). The R_s refers mainly to the bulk electrolyte solution resistance and the intrinsic resistance of active material. The R_{ct} indicates the kinetic resistance to charge transfer at electrode/electrolyte interface. The value of CPE is a function of the angular frequency (ω) and its phase is independent of the frequency. The admittance and impedance of the CPE can be described as follows:

$$Y_{\mathrm{CPE}} = Y_0(j\omega)^n \quad (2)$$

$$Z_{\mathrm{CPE}} = \frac{1}{Y_0(j\omega)^{-n}} \quad (3)$$

where Y_0 is the magnitude of the CPE and *n* is the exponential term of the CPE [16]. The CPE has been widely used to fit impedance spectra for Cu in CMP slurries [17,18]. Some studies have claimed that the *n* value approaching to unity reflects a more homogeneous Cu surface and thus yields Cu electrode with a reduced roughness [19-21].

The best-fit impedance parameters for these results are illustrated in Table 1. In comparison with BTA passive film at 0.3 V vs. Ag/AgCl, ATRA passive film possessed larger R_{ct} values and smaller CPE values. The decrease in the CPE values which may originate from a decrease in the local dielectric constant and/or an increase in the thickness of double layer was attributed to the gradual replacement of water molecules and other ions originally adsorbed on the surface of electrode [22-24]. The impedance spectrum shown in Fig. 3a for BTA passive film at 0.5 V vs. Ag/AgCl does not fit here due to its somewhat unusual shape displaying a highly depressed semicircle at intermediate frequency and a nearly vertical line at low frequency. Nevertheless, the magnitude of the real impedance dropped

considerably when the applied anodic potential was increased to 0.5 V vs. Ag/AgCl, which was much less in comparison with that of the ATRA passive film.

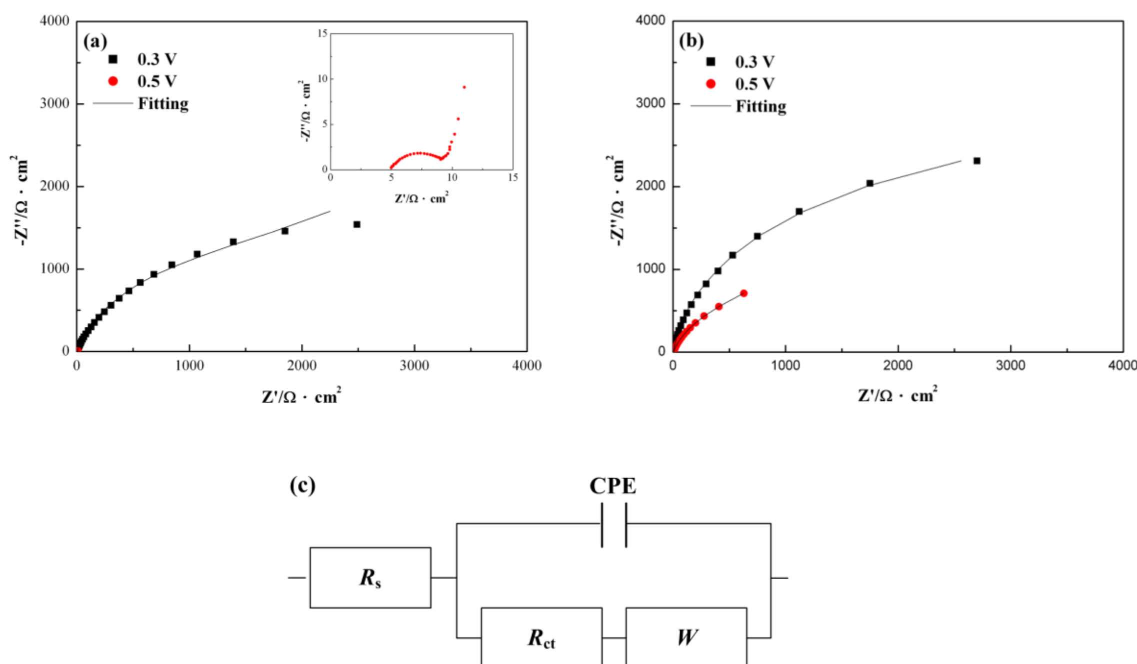

Figure 3. Nyquist impedance plots for phosphate electrolytes containing (a) 0.01 M BTA, (b) 0.01 M ATRA. (c) Equivalent circuit model for Cu corrosion. Prior to EIS measurements, Cu foils were immersed in the desired electrolyte for 30 min. The interplot of Fig. 3a is the enlargement of 0.01 M BTA at 0.5 V vs. Ag/AgCl.

Table 1. Best-fit values for R_s, R_{ct}, Y_0, n, and W of the equivalent circuit in Fig. 3c to the impedance spectra in Figs. 3a and 3b.

	Operating potential (V vs. Ag/AgCl)	R_s (Ωcm^2)	R_{ct} (Ωcm^2)	Y_0 ($\mu F\ cm^{-2}$)	n	W ($\mu\Omega\ cm^2$)
BTA passive film	0.3	4.3(0.12)	2063(129)	3.315 (0.150)	0.860(0.005)	68.3(6.1)
ATRA passive film	0.3	5.0(0.03)	3286(86)	2.841 (0.039)	0.940(0.001)	68.3(3.8)
ATRA passive film	0.5	5.0(0.02)	1139(40)	19.67(0.252)	0.843(0.001)	166.0(7.8)

Consequently, the protective nature of the ATRA passive film was clearly inferred by the fact that the inhibition capability against Cu dissolution was superior to that of the BTA passive film, especially at higher operating potentials. Indeed, this finding is accordance with the voltammetric results. Moreover, the n value for BTA passive film at 0.3 V vs. Ag/AgCl was 0.860, which was much

smaller than that for ATRA passive film. This implies that the homogeneous Cu surface or the reduced surface roughness can be obtained in the presence of ATRA.

3.3 Morphologies of passive films

To characterize the passive films forming on the Cu surface, AFM analyses were performed. Figures 4a and 4b show AFM images of remaining inhibitor layers adsorbed on Cu surfaces (5 × 5 μm) after exposing to the phosphate electrolytes with 0.01 M BTA and 0.01 M ATRA at 0.3 V vs.Ag/AgCl for 150 s and then subjected to rising by DIW solution, respectively. It is noticeable that the BTA passive film forming on the Cu surface shows a larger granular structure compared to that of ATRA passive film. It is possible that ATRA stands up lengthwise on the Cu surface and thus makes a denser passive film than BTA, resulting in the lower surface roughness of 10.74 ± 2.24 nm. This observation regarding the reduced surface roughness in the presence of ATRA, due to denser self-aligned film, is consistent with the EIS results. The enhanced passivation capability of ATRA could in part be attributed to this denser passive film.

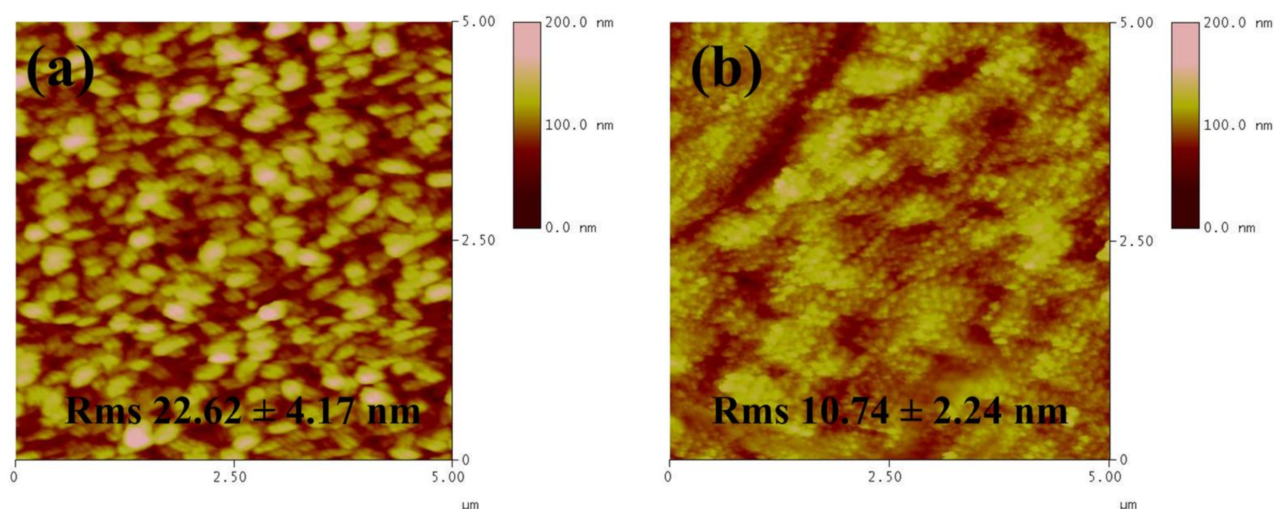

Figure 4. 5 μm × 5 μm ex situ tapping mode 3D AFM images of Cu foils. (a) and (b) after treating in phosphate electrolytes containing 0.01 M BTA and 0.01 M ATRA at a constant potential of 0.3 V vs. Ag/AgCl for 150 s.

3.4 Polishing performance

To evaluate whether ATRA can be used for the phosphate ECMP process, a Cu patterned structure was employed. Figure 5 shows the planarization results of patterned Cu foils for the phosphate electrolyte containing 0.01 M ATRA at an operating potential of 0.7 V vs. Ag/AgCl under a downward force of ~0.5 psi. Representation profilometric scans recorded before and after polishing were superimposed on top of one another in Fig. 5. An apparent step height reduction value of ~800

nm was achieved after polishing. Additionally, the surface quality for the up area of patterned Cu foil before and after the ECMP process was characterized by means of AFM measurements, as shown in Fig. 6. It can be noted that no obvious increase in surface roughness is observed after ECMP process. These results indicate that the ATRA-containing phosphate electrolyte can be used for ECMP process, especially in the case of higher anodic potential.

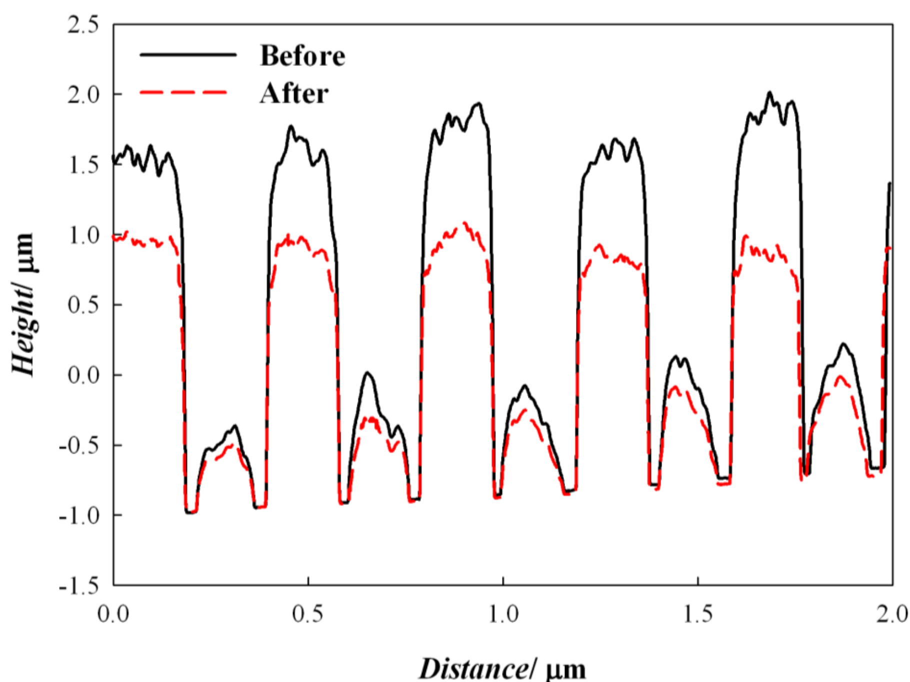

Figure 5. Profilometry scans of a patterned Cu foil before and after polishing with an IC1000™ pad for 60 s in phosphate electrolytes containing 0.01 M ATRA at 0.7 V vs. Ag/AgCl.

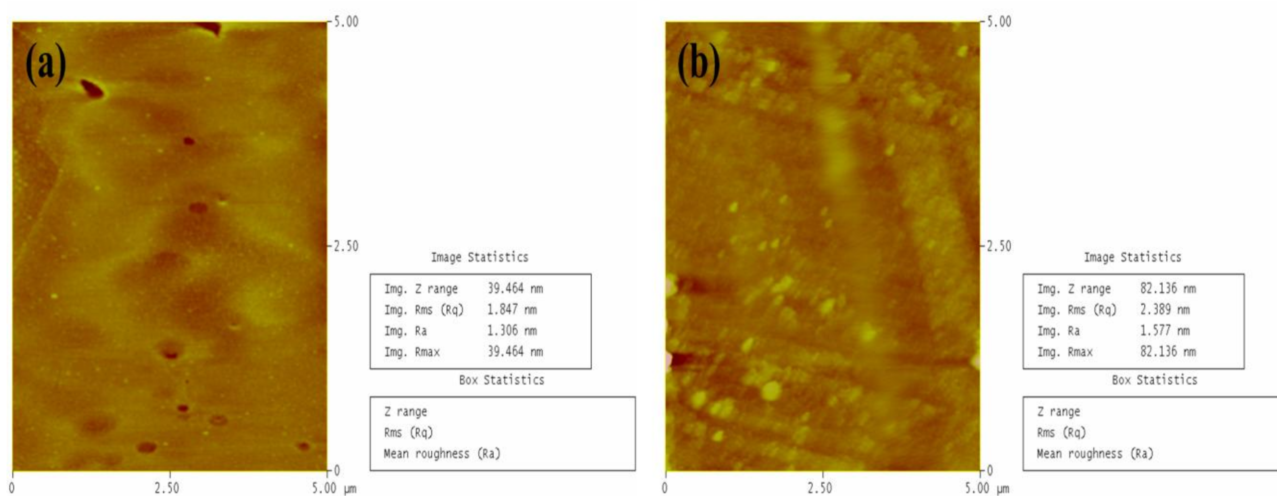

Figure 6. 5 µm × 5 µm ex situ tapping mode 3D AFM images obtained (a) before and (b) after ECMP process in a phosphate electrolyte containing 0.01 M ATRA at a constant applied potential of 0.7 V Vs. Ag/AgCl for 60 s.

4. CONCLUSIONS

A phosphate electrolyte for Cu ECMP containing 0.01 M ATRA was studied using electrochemical measurements, AFM analysis and polishing of blanket and patterned Cu foils. It was found that the ATRA passive film was likely to possess a superior passivation capability to BTA passive film, especially at higher anodic potential. The enhanced passivation of ATRA was mainly attributed to the denser possible passive film originating from ATRA compounds. In addition, the results of polarization curves with and without abrasion further predicted that a potential window (~ 0.4 V) within which the ε_{ECMP} and the Cu removal rate were greater than 70% and 600 nm min^{-1}, respectively. Furthermore, the ECMP experiment on a patterned Cu foil demonstrated that an apparent step height reduction of ~800 nm can be achieved in the phosphate electrolyte consisting of 0.01 M ATRA at such high potential of 0.7 V vs. Ag/AgCl for only 60 s. The higher removal rate was achievable in the presence of ATRA compared to BTA with equivalent planarization results, thus driving shorter polishing time to balance polishing steps in a serial mode over multiple platens. This increased removal rate could be helpful with throughput and corrosion defectivity reduction during the planarization process.

ACKNOWLEDGMENTS
The authors are very grateful to the National Science Council in Taiwan for its financial support under Contract No. NSC-98-2218-E-036-002. We also thank Tatung University in Taiwan, under the grant B98-C11-010, for partial financial support.

References

1. I.I. Suni, B. Du, *IEEE Trans. Semicond. Manuf.*, 18 (2005) 341.
2. D. Truque, X. Xie, D. Boning, *Mater. Res. Soc. Symp. Proc.*, 991 (2007) 315.
3. F.Q. Liu, T. Du, A. Duboust, S. Tsai, W. Hsu, *J. Electrochem. Soc.*, 153 (2006) C377.
4. Y. Oh, G. Park, C. Chung, *J. Electrochem. Soc.*, 153 (2006) G617.
5. A. Tripathi, C. Burkhard, I.I. Suni, Y. Li, F. Doniat, A. Barajas, J. McAndrew, *J. Electrochem. Soc.*, 155 (2008) H918.
6. K.G. Shattuck, J.Y. Lin, P. Cojocaru, A.C. West, *Electrochim. Acta*, 53 (2008) 8211.
7. J.Y. Lin, A.C. West, *Electrochim. Acta*, 55 (2010) 2325.
8. J.Y. Lin, A.C. West, C.C. Wan, *J. Electrochem. Soc.*, 155 (2008) H396.
9. Q. Luo, S.V. Babu, *J. Electrochem. Soc.*, 147 (2000) 4639.
10. S. Jeong, S. Joo, H. Kim, S. Kim, H. Jeong, *Jpn. J. Appl. Phys.*, 48 (2009) 066512.
11. J.W. Lee, M.C. Kang, J.J. Kim, *J. Electrochem. Soc.*, 152 (2005) C827.
12. S.A. Umoren, I.B. Obot, E.E. Ebsenso, N.O. Obi-Egbedi, *Int. J. Electrochem. Sci.*, 3 (2008)1029.
13. J.Y. Lin, A. C. West, C.C. Wan, Y.Y. Wang, *Electrochem. Commun.*, 10 (2008) 677.
14. J.Y. Lin, S.W. Chou, *Electrochim. Acta*, 56 (2011) 3303.
15. K.G. Shattuck, A.C. West, *J. Appl. Electrochem.*, 39 (2009) 1719.
16. W. Scheider, *J. Phys. Chem.*, 79 (1995) 127.
17. E.M. Cafferty, *Corros. Sci.*, 39 (1997) 243.
18. M. Touzet, M. Cid, M. Puiggali, M.C. Petit, *Corros. Sci.*, 34 (1993) 1187.
19. Y.F. Wu, T.H. Tsai, *Microelectron. Eng.*, 84 (2007) 2790.
20. T.H. Tsai, Y.F. Wu, S.C. Yen, *Microelectron. Eng.*, 77 (2005) 193.

21. H. Ashassi-Sorkhabi, D. Seifzadeh, *Int. J. Electrochem. Sci.*, 1 (2006) 92.
22. M. Behpour, S.M. Ghoreishi, N. Soltani, M. Salavati-Niasari, M. Amadanian, A. Gandomi, *Corros. Sci.*, 50 (2008) 2172.
23. J. Aljournai, K. Raeissi, M.A. Golozar, *Corros. Sci.*, 51 (2009) 1836.
24. A.K. Singh and M.A. Quraishi, *Corros. Sci.*, 51 (2009) 2752.

© 2012 by ESG (www.electrochemsci.org)